Biosensors and Bioelectronics: X 14 (2023) 100344

Contents lists available at ScienceDirect

Biosensors and Bioelectronics: X

journal homepage: www.journals.elsevier.com/biosensors-and-bioelectronics-x

Fuel cells operating as an immunosensor for cancer biomarker screening

Nádia S. Ferreira [a,b,c,d], Liliana P.T. Carneiro [a,b,c,d], Alexandra M.F.R. Pinto [c], M. Goreti F. Sales [a,b,d,*]

[a] BioMark@ISEP, School of Engineering, Polytechnic Institute of Porto, Portugal
[b] BioMark@UC, Department of Chemical Engineering, Faculty of Sciences and Technology, University of Coimbra, Portugal
[c] CEFT, Department of Chemical Engineering, Faculty of Engineering, University of Porto, Portugal
[d] CEB, Centre of Biological Engineering, Minho University, Portugal

ARTICLE INFO

Keywords:
Immunosensor
Direct methanol fuel cell
CA15-3
Cancer biomarker
Point-of-care

ABSTRACT

This work presents the first integration of antibodies into one of the electrodes of a passive direct methanol fuel cell (DMFC) to create an autonomous immunosensor for cancer antigen 15–3 (CA15-3). The anode of the fuel cell was first made of carbon cloth with carbon black, platinum and ruthenium nanoparticles and then modified with anti-CA15-3, while the cathode was made of carbon cloth with carbon black and platinum nanoparticles. This hybrid DMFC (hDMFC), which works as an immunosensor, was fed with dilute methanol to generate a concentration-dependent current.

The hDMFC device was calibrated in different media (buffer and serum), by incubating increasing concentrations of CA15-3 standard solutions, ranging from 47 to 750 U/mL. The linear response ranged from 188 to 563 U/mL, and the limit of detection (LoD) was 39.8 U/mL. The selectivity of the biosensor was also evaluated with competing cancer biomarkers, such as carcinoembryonic antigen (CEA), and cancer antigen 125 (CA-125), as well as with other compounds normally present in blood plasma (ascorbic acid, glucose, uric acid and urea), adjusted to the normal range of concentrations in serum. The results obtained indicate good selectivity of the immunosensor in the fuel cell.

In general, the immunosensor showed a good response considering its integration into a passive DMFC. It is a good sensor for point-of-care (PoC) diagnosis because it has a good performance in human serum and, most importantly, it pursues electrical autonomy.

1. Introduction

Biosensor research dates back several decades and has now established itself as a growing area of interest for point-of-care (PoC) health monitoring. These are analytical devices that convert a response obtained through a biological or biomimetic material - biorecognition element - into a measurable electrical signal-transducer (Mehrotra, 2016). The need for PoC biosensors is increasing day by day and is becoming more and more important for quick, easy, and cost-effective screening of various diseases. In response to the specific needs of underdeveloped countries and in case of global crisis or war scenarios, it is important that biosensors can operate autonomously and use readily available energy.

In search for autonomous devices, some research works make use of microbial fuel cells (Pasternak et al., 2017), enzymatic fuel cells (Gonzalez-Solino and Di Lorenzo, 2018), Dye-sensitized solar cells (Truta et al., 2018) or Direct Methanol Fuel Cells (DMFCs) (Sales and Brandão, 2017). Although these approaches offer autonomy features, microbial and enzymatic fuel cells are very delicate systems that require specific conditions of operation and have difficulties in terms of reproducibility, limiting their application to quantitative measures. Moreover, dye-sensitized solar cells (DSSCs) are not functional at night limiting their operation in places where there is no electrical power.

A power source that favours the operation of autonomous biosensors at any time and with higher performance are DMFCs. DMFCs convert chemical energy into electrical energy and are now widely used, including in commercial applications. These cells are simple, environmentally friendly, highly efficient, reliable, have a long lifetime and can be easily miniaturized. They use methanol as fuel, which can be easily stored and transported compared to hydrogen-fed fuel cells, which

* Corresponding author. Department of Chemical Engineering, Faculty of Sciences and Technology, University of Coimbra, Rua Sílvio Lima, Polo II, 3030-790, Coimbra, Portugal.
E-mail addresses: goreti.sales@gmail.com, goreti.sales@eq.uc.pt (M.G.F. Sales).

https://doi.org/10.1016/j.biosx.2023.100344
Received 10 December 2022; Received in revised form 27 February 2023; Accepted 19 March 2023
Available online 13 April 2023

simplifies the fuel cell system (Liu et al., 2006). In addition, they offer high power, meaning that only a small volume of methanol (few mL) is enough for their operation. To date, DMFCs have been interfaced with plastic antibodies as biorecognition layer (Carneiro et al., 2021, 2022; Ferreira et al., 2022; Sales and Brandão, 2017) but no work has been conducted with antibodies, which in general are a guarantee of the production of a selective response.

Thus, this work presents for the first time a combination of antibodies and DMFCs aimed at producing an autonomous immunosensor. This principle was applied to cancer antigen 15–3 (CA15-3), a cancer biomarker circulating in the blood. Healthy individuals contain 25 U/ml of CA15-3 (Ebeling et al., 2002), and higher levels indicate a cancer diagnosis, including breast cancer, the most common cancer in women worldwide (Globocan and Global Cancer Observatory, 2020). To date, there are several biosensors for the determination of CA15-3. These include various concepts and approaches, many of which are electrochemical (Perfézou et al., 2012; Soper et al., 2006; Tavares et al., 2016; Tothill, 2009), optical (Chen and Wang, 2020), or lateral flow assays (Bayoumy et al., 2020; Di Nardo et al., 2021; Mahmoudi et al., 2020). Electrochemical sensors offer high sensitivity but are electrically powered devices, thereby being energy dependent. This limits their use to locations where a power source is available, which may not always be the case. Excluding coloured systems detected by naked eye, optical sensors are also powered by an electrical device to measure the generated signal (Naresh and Lee, 2021). Lateral flow assays are energy independent, but they provide a simple "yes" or "no" response and are not able to quantify the concentration of the biomarker, which is important in this case to determine whether a particular individual has a normal or high CA15-3 level.

In detail, this work describes the design of a hybrid DMFC system (hDMFC) consisting of two carbon-based electrodes on commercial carbon cloth, one of which is modified with antibodies against CA15-3. In this way, the performance of the cell becomes concentration dependent, because when more CA15-3 is bound to the antibodies, less energy is generated by the hDMFC. The system was optimised with respect to key variables and calibrated under buffered conditions to define the linear reaction range and detection limit (LoD) of the hDFMC. Selectivity studies and calibration in serum-based solutions were also performed to anticipate the behaviour of the hDMFC under realistic conditions.

2. Results and discussion

2.1. Assembly of the immunosensor electrode

The immunosensor electrode was constructed as described in the experimental section (Supplementary data), corresponding to the scheme shown in Fig. 1, having each modification step followed by a three-electrode system with a ferrocyanide redox probe and EIS measurements. The first step of the modification consisted of the addition of cysteamine, which binds to the Pt nanoparticles. This binding decreases the intrinsic conductivity properties of Pt, leading to an increase in charge transfer resistance. The positive charge on the surface generated by the cysteamine could also have reduced the resistance to charge transfer of the negatively charged probe, but this effect was less pronounced than the effects on reducing the conductivity properties of Pt. Then the activated antibodies, previously modified with EDC/NHS chemistry, were added to the electrode with the amine layer. The activated carboxyl groups were capable of mild reaction with the amine groups and covalently bound the antibodies to the electrode surface. This modification contributed to an additional increase in resistance. Deactivation of the activated carboxylic groups that did not react was necessary to stabilize the electrode, and this was done by adding ethylenediamine. Since ethylenediamine carries positively charged amino groups, the resistance to charge transfer of the negatively charged probe decreased. The final step of the modification was the addition of BSA to

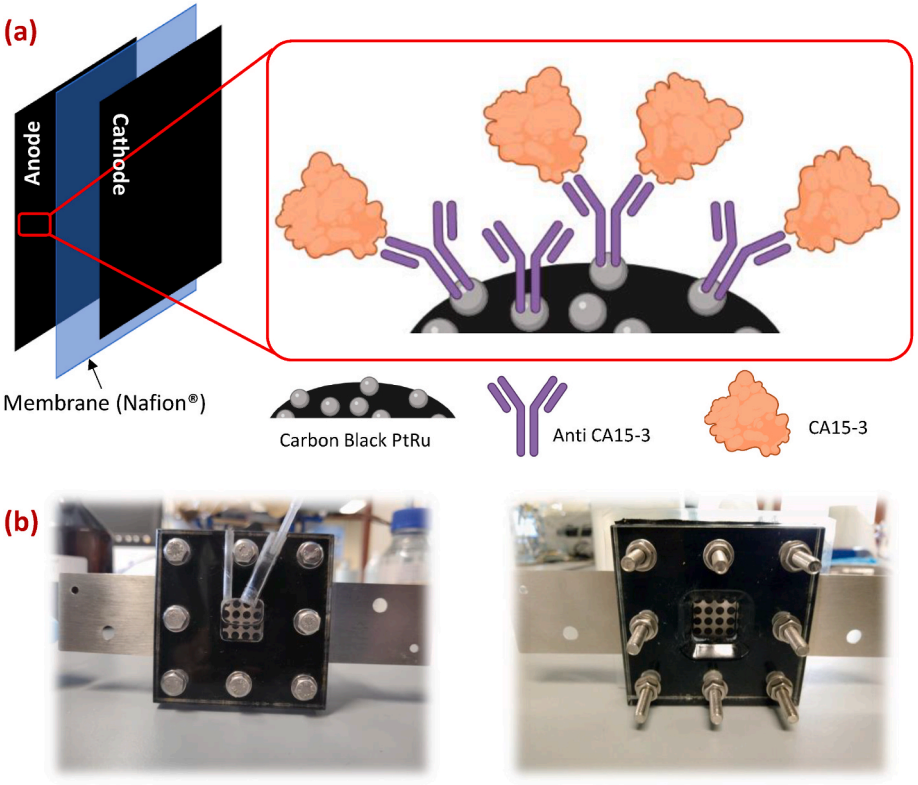

Fig. 1. (a) Schematic representation of the immunosensor assembly: integration of the immunosensor on the anode of the Membrane Electrode Assembly (MEA) from the passive Direct Methanol Fuel Cell (DMFC); **(b)** Real passive DMFC that was used throughout this work, where the immunosensor was assembled.

reduce the nonspecific binding of CA15-3 to the electrode surface. The presence of BSA contributed to an additional increase in resistance to charge transfer (Fig. S1). Overall, these results showed a similar trend to a previous immunosensor construction using a similar strategy (Ferreira and Sales, 2014), indicating that the immunosensor was successfully constructed. The amplitude of the observed resistance changes was smaller than when an immunosensor was built on commercial carbon electrodes, but this was already observed by us when Pt nanoparticles were added to these commercial carbon electrodes.

2.1.1. SEM and EDS analysis

Fig. S2 shows the results of SEM (Figs. S2a and b) and EDS (Figs. S2c and d) analysis of the Carbon Cloth/PtRu carbon black electrode before (Fig. S2a) and after modification with the antibody (Fig. S2b). As expected, the SEM images showed different light contrasts (Brodusch et al., 2018; Wells et al., 2006), because when the platinum is more exposed (control sample – Fig. S2a) the brightness is more intense than when the antibody is bound to the platinum nanoparticles (Fig. S2b). These differences in image contrast indicate that a change has occurred at the electrode, due to the attachment of the antibody to the platinum on the electrode surface. When analysing the EDS spectra (Figs. S2c and d), the control sample shows similar results to previous studies (Nashner et al., 1997; Zhang and Chan, 2003) with high Pt and Ru element peaks, mostly between 2 and 3 keV. For the electrode with the antibody, a slight increase in nitrogen (N) is observed in the modified sample. This indicated that an increased amount of this component was present, due to the presence of the amino groups (-NH_2) of the antibody and the cysteamine on the surface. Overall, the data obtained confirmed the modification of the electrode, both in terms of image contrast and changes in EDS.

2.1.2. Raman spectroscopy

When excited at a wavelength in the visible region of the Raman spectrum, both D and G bands are typically found in graphite spectra, and the D band indicates defects or disorder in the carbon structure. Quantification of disorder is obtained by calculating the ratio between the G (related to the sp^2 carbon bonding) and D (related to the sp^3 carbon bond) bands (I_D/I_G) (Dresselhaus et al., 2010; Jawhari et al., 1995). Looking at the overall spectra, the Raman intensity was low compared to similar spectra from carbon black only, which was already expected (Cerezo-Navarrete et al., 2021). This was consistent with previous studies of the group, which indicated that the presence of Pt/Ru was quenches the Raman signal. In terms of I_D/I_G ratio, there are small differences between the immunosensor assembly steps (Fig. S3). Since the overall intensity was low, it meant that the assembly of the immunosensor was successful, which is consistent with the SEM and EIS data.

2.2. Selection of methanol concentration

An optimally functioning passive DMFC using the same design as in this work achieves power densities and currents around 2.5 mW/cm^2 when operated at high methanol concentrations (3–4 M) (Berns et al., 2015; Carneiro et al., 2021). These high concentrations ensure that the cell also delivers the maximum possible energy because the amount of methanol is in excess compared to what can be consumed by the cell. However, while high concentrations promote high electrical output from the cell, high methanol concentrations can compromise the quality of the hDMFC analytical response for two reasons. One reason is that if the cell is operated with an excess of methanol, it will not detect when a small amount of methanol has not reached the PtRu particles, making it insensitive to CA15-3 binding. The other reason is the possible denaturation of the antibody in the presence of a large amount of methanol, which in turn impairs the ability of the antibody to bind its target antigen. Therefore, in order to maintain the antibody-antigen reaction and ensure electrical autonomy and operational sensitivity, a medium methanol concentration had to be used. In addition, two methanol concentrations should be considered, one for the activation phase and the other for the operation of the cell. In this work, methanol was not in direct contact with the serum that was incubated in the fuel cell, since the reservoir was thoroughly washed with water between each step, leaving, only the antibody and antigen in direct contact with methanol. However, there are already some studies regarding the denaturation of proteins in methanol mixtures (with water or with other solvents) that show little effect of methanol on proteins conformation on concentrations lower than 25–30% (v/v), ~6 M (Babu and Douglas, 2000; Fernández and Sinanoğlu, 1985; Shao, 2014; Yamazaki et al., 2006), indicating that our molecules are not denatured in the low methanol concentrations used in this work.

In previous studies 0.05 M of methanol was shown to be the best performing methanol concentration to achieve a functional and sensitive biosensor, which is why in this work this concentration was firstly tested. Since 0.05 M methanol was not enough to power the DMFC with the immunosensor, 0.1 M methanol was therefore tested to obtain the achieved results. It was the minimal methanol concentration to be used for DMFC powering without losing the biosensor response (Carneiro et al., 2022).

Initially, the DMFC was activated with a methanol concentration of 0.5 M. This activation is done by leaving the fuel cell with the methanol solution for several hours (3–4 h), so that the liquid penetrates through the fibers of the carbon fabric and starts to react with the platinum particles. Then several sampled DC measurements were performed until the stability of the system was reached. Higher concentrations lead to an excessive amount of methanol adsorbed on the electrodes, which is subsequently very difficult to remove.

The performance and difference between an unmodified and a modified cell after the first activation (with 0.5 M) are shown in Fig. S4. Fig. S4a shows a clear difference in the starting potential of the cell with or without the immunosensor electrode. The presence of the sensor material at the anode hindered the access of methanol to the platinum and consequently the initial OCP and power densities were lower than for the unmodified cell (Fig. S4b). After completing fuel cell activation with 0.5 M methanol, the excess was removed by filling the anode reservoir with Milli-Q water overnight. As a result, the fuel cells had near zero OCP at the start of calibration.

At this point, a compromise had to be made between fuel cell performance and a sensitive biosensor for methanol concentration during calibration. The methanol concentration had to be high enough for the fuel cell to provide consistent performance and stable readings, but low enough to ensure antibody activity and selectivity. To find the best compromise, two different methanol concentrations were tested: 0.050 and 0.10 M. At 0.05 M, the fuel cell showed no response and kept its OCP close to zero, as at startup (Fig. S5a). When 0.10 M methanol was used, the cell began to produce energy until stable readings were obtained (Figs. S5b and c). Since the fuel cell did not generate current signals when 0.05 M was used, a concentration of 0.1 M methanol was used in the calibrations in this work.

2.3. Calibrations in buffer

The calibration of the system consisted in incubating consecutively standard solutions of increasing concentration and checking the electrical output of the hDMFC. After each incubation, the system reservoir was washed with ultra-pure water and the measurements of sampled DC were performed using the selected methanol solution. To be sure that the hDMFC was providing stable readings, various incubations in measuring buffer were performed first (three to four times), until a stable response was achieved. Having standard solutions prepared in MES buffer, the first incubations were made with MES. About 3 to 4 incubations were necessary prior to calibration.

Several calibrations of CA15-3 were performed with independent electrodes to determine the typical analytical characteristics of the

calibration of hDMFC. The typical data obtained in one calibration run of the sample DC are shown in Fig. 2a and the calibration curve is shown in Fig. 2b, where the normalized values of the power density of hDMFC are plotted against the log concentration of CA15-3 (U/mL) and each standard of each concentration value (in the form of error bars). The lower concentrations of CA15-3 are able to reduce the power signal, but not with sufficient sensitivity to produce a linear trend. The linear trend is observed only from 281.5 to 750 U/mL. The average power density changed within this linear range from 0.078 to 0.042 mW/cm^2, with this last value obtained by incubating the highest protein concentration. This corresponded to a deviation of about 54% between the initial and final power output, which was consistent across the different calibrations with buffered standard solutions. This decrease in power with increasing CA15-3 concentration reflects decreasing methanol oxidation at the platinum surface. The increasing number of CA15-3 proteins bound to the antibody increases the steric hindrance of methanol at the metal catalyst. This decreases the power generated by the cell as the electron flow is restricted by the external circuit.

The representative calibration curve obtained by normalizing the power curve values (power sample/power blank) had a slope of −0.6105 and a squared correlation coefficient (R^2) of 0.9773, as shown in Fig. 2b. The system was highly reproducible, with standard deviations of individual standards ranging from 0.04% to 5.0%. The detection limit achieved was 39.8 U/mL.

2.4. Calibrations in Cormay® serum

To verify the functionality of the fuel cell integrated immunosensor in the analysis of human samples, CA15-3 standard solutions were prepared in diluted Cormay® serum. This is a commercially available human serum that can be used to evaluate the effects of a real serum on the operation of the immunosensor. The high quantity of salts and ions present in this matrix made it difficult to test this sample and avoid poisoning of the catalyst and membrane of the fuel cell. Therefore, this serum was 1000x diluted in MES buffer, to minimize the poisoning of the system due to the small molecules that are not of interest for our biosensor. The concentrations of CA15-3 used for this purpose ranged from 46.8 to 750 U/mL. The results obtained are shown in Fig. 3. Comparing the slopes obtained in the two tested media is observed a slight decrease in the sensitivity of the system in the Cormay® serum media. The analysis of the calibrations performed in buffer showed that the final signal output decreases by ~50% (compared to the initial value after stabilisation of the background medium) towards the maximum concentration of CA15-3, while in Cormay® serum the signal output decreases by ~ 70%. Since Cormay® serum is a more complex matrix in comparison with buffer, these results demonstrate that this DMFC sensor keeps a good performance and sensitivity in more complex matrices, making it suitable for application in real samples. In this case, the initial concentrations of CA15-3 used in the calibrations showed no or very little response and an initial plateau, followed by a decreasing in the power of the fuel cell as the standard concentration was increased, with linear response from 187.5 to 750U/mL. The system was also highly reproducible when calibrated with this sample, resulting in low standard deviations between 1.1% and 3.6%.

2.5. Analytical recovery

Recovery is defined by IUPAC as the “Proportion of the amount of analyte, present in or added to the analytical portion of the test material, which is extracted and presented for measurement” (Thompson et al., 1999). In electrochemical sensors this is usually estimated by spiking, meaning that known amounts of analyte are added to the blank or suitable medium. These are then analysed an unspiked portion of the medium. The difference of these two allows to estimate the recovered part of the added analyte. This is called the “surrogate recovery” (Desimoni and Brunetti, 2013; Moretto. et al., 2015).

In this work the analytical recovery was determined by the surrogate recovery, by spiking buffer and Cormay® serum with known amounts of analyte. The obtained calibration curves were then used to calculate the % of recovery that are shown in Table 1. The immunosensor shows a good performance in detection of CA15-3 with a very good recovery values (ranged from 98.5% to 104.7%) suggesting the possibility of the proposed sensor for real sample analysis.

2.6. Selectivity studies

To evaluate the selectivity of the immunosensor response, tests were performed in which potentially interfering species that may be present in human serum (at biological concentrations) were added to a known concentration of CA15-3. This selectivity study was made against common species in serum, such as glucose and ascorbic acid, and other cancer biomarkers, such as CA125 and CEA. For this purpose, different independent fuel cells were assembled and tested with different species: a known CA15-3 concentration and the same known CA15-3

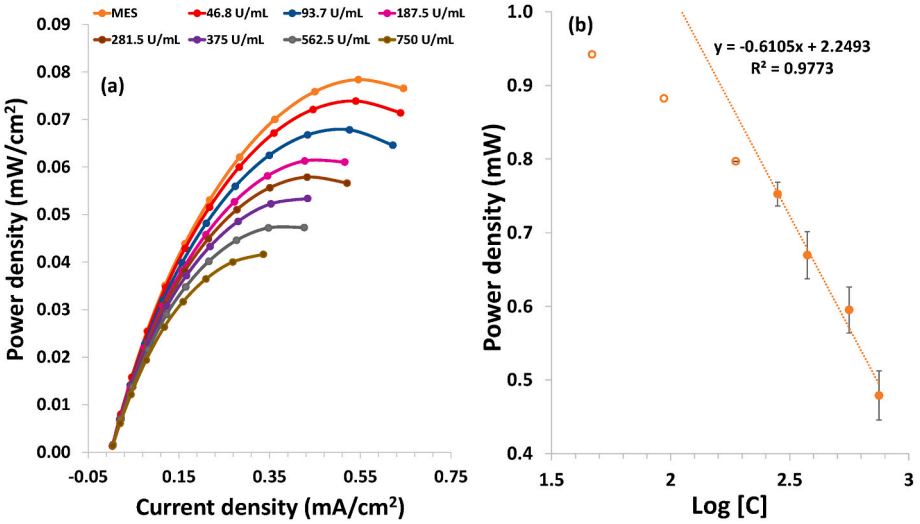

Fig. 2. **(a)** Representation of a typical calibration plot obtained from the polarization curves from the Fuel Cell when using MES buffer as medium; **(b)** Calibration curves with normalized values of the obtained power curves of the modified fuel cells and its respective standard deviation (error bars; $n = 3$). Standards from 46.8 U/mL to 750 U/mL of CA15-3 in MES buffer were used.

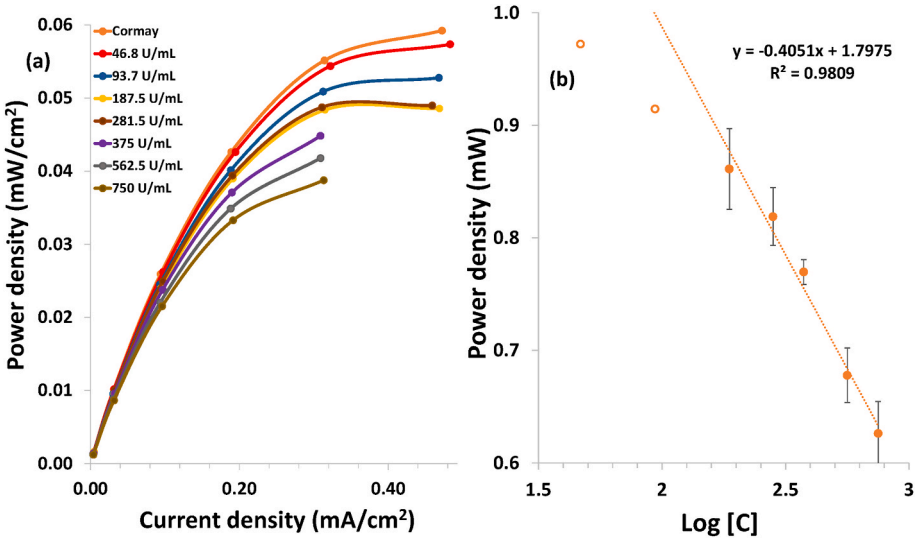

Fig. 3. (a) Representation of a typical calibration plot obtained from the polarization curves from the Fuel Cell when using Cormay® serum as medium; **(b)** Calibration curves, obtained with Cormay® serum, with normalized values of the obtained power curves of the modified fuel cells and its respective standard deviation (error bars; $n = 3$). Standards from 46.8 U/mL to 750 U/mL of CA15-3 in serum were used.

Table 1
Recovery study in Buffer and Cormay® serum calibrations.

Buffer			Cormay® serum		
Added CA15–3 (U/mL)	Calculated CA15-3 (U/mL)	% Recovery	Added CA15-3 (U/mL)	Calculated CA15-3 (U/mL)	% Recovery
187.50	239.4	104.7	187.5	204.9071401	101.7
281.50	283.1	100.1	281.5	260.5137989	98.6
375.00	387.0	100.5	375	344.7162419	98.6
562.50	512.3	98.5	562.5	580.7453769	100.5
750.00	794.3	100.9	750	778.9027682	100.6

concentration spiked with an interfering substance (one fuel cell for each interfering substance). The concentrations of each interfering cancer biomarker was high, implying illness, concentrations that would be found in a cancer patient: 100 ng/mL CEA, and 150 U/mL CA125. For the interferents that are a part of the human blood, the used concentrations were within the normal range in the blood: 1.3 mg/mL glucose, 0.02 mg/mL ascorbic acid, 0.2 mg/mL urea, and 0.06 mg/mL uric acid.

As expected, the results reveal the selectivity of the immunosensor for CA15-3, with the interfering substance changing the signal between 0.7 and 5.9. Fig. 4 shows the influence of the interfering species on the fuel cell signal, with the smallest influence observed in the analysis with ascorbic acid (0.7% decrease in signal compared to control - fuel cell with only CA15-3 standard). The interfering species that had a greater effect on fuel cell power output was the use of CA125 (5.9% increase in signal) and urea (5.2% increase in signal), which can be explained by the similarity of CA125 to CA15-3 in terms of structure, since they are both members of the mucin family glycoproteins. Urea is an interfering species for this system, since it also is used in electrocatalysis, and can be used as fuel in fuel cells with platinum catalyst. Therefore, it is expectable to have a change in fuel cell power when adding urea to the system (Xu et al., 2016). CEA was also tested and had a minor effect on fuel cell power output (2.2% decrease in signal). Overall, these results show that the interfering species had a small effect on fuel cell performance.

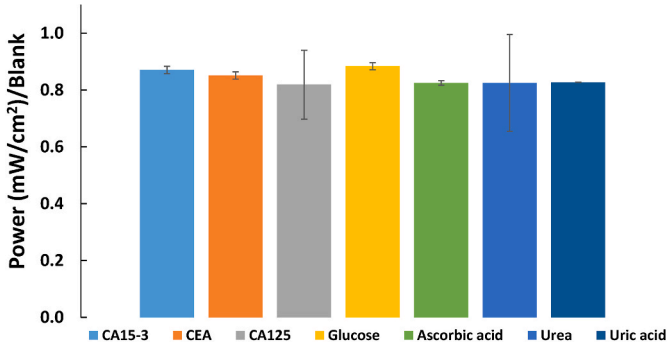

Fig. 4. Response of the immunosensor for potential interfering species: other cancer biomarkers (CA125, CEA) and common interfering substances found in the Human serum (ascorbic acid, glucose). All values were normalized against the blank (MES buffer), and standard deviation (error bars; $n = 2$) were added for each interfering species.

2.7. Comparison to previous CA15-3 biosensors

Some biosensors from the literature targeting the detection of CA15-3 were used for comparison with this work. Table 2 lists other electrochemical immunosensors from recent years and their differences from this work. Although we can see that the analytical performance of the other immunosensors is superior to this work (LoD values and linear response), this work has a broader linear range for CA15-3 concentrations, and this range includes the concentration of interest in the clinical setting (patients with cancer). Another novel feature of this work is the ability to turn the system into an autonomous sensor, which has the great advantage of being able to be used anytime, anywhere, without the need for power or other devices. The potential autonomy and response to the biomarker CA15-3 in the clinical setting are beneficial for PoC analysis.

3. Conclusions

In conclusion, the hDMFC exhibits a concentration-dependent

Table 2
Other works reporting electrochemical immunosensors for CA15-3 determination in the literature.

Support	Autonomy	Linear response	LOD	Reference
rGO and CuS placed on a SPGE	No	1.0–150 U/mL	0.3 U/mL	Amani et al. (2018)
CysA/GQDs	No	0.16–125 U/mL	0.11 U/mL	Hasanzadeh et al. (2018)
CoS_2-GR and AuNPs composites	No	0.1–150 U/mL	0.03 U/mL	Khoshroo et al. (2018)
Dual SPCE	No	0 to 70 U/mL	5.0 U/mL	Marques et al. (2018)
Gold electrode	No	15–50 μU/mL	15 μU/mL	Akbari Nakhjavani et al. (2018)
Graphite ink	No	15–250 U/mL	15 U/mL	Saadati et al. (2019)
Cu-MOF	No	10 μU/mL to 10 mU/mL 10 mU/mL to 100 U/mL	5.06 μU/mL	Zhang et al. (2019)
Gold electrode	No	1–1000 U/mL	0.95 U/mL	Rebelo et al. (2021)
Graphite-based ink	No	0.5–200 U/mL	0.15 /mL	Hosseinzadeh et al. (2022)
Carbon with PEI-AuNPs	No	0.10–100 U/mL	0.21 U/mL	Kuntamung et al. (2021)
GCE with Ag/TiO_2/rGO	No	0.1–300 U/mL	0.07 U/mL	Shawky & El-Tohamy et al. (2021)
CBPtRu	Yes	187.5–562.5 U/mL	39.8 U/mL	This work

Au-NPs: Gold nanoparticles; **CBPtRu:** Carbon Black with Platinum and Ruthenium nanoparticles; **Cu-MOF:** Copper-based metal-organic framework nanoparticles; **CysA/GQDs:** thiolated graphene quantum dots; **GCE**: Glassy carbon electrode; **PEI**: Polyethylenimine; **rGO:** Reduced Graphene Oxide; **SPCE:** Screen Printed Carbon Electrode.

response to the presence of the target molecule, such that the fuel cell can be used as an autonomous sensing device in conjunction with an electrochromic device that changes colour in the presence of the target analyte. This was demonstrated by using different background media and assessing the selectivity of this sensor with molecules in blood plasma and other relevant cancer biomarkers. The results obtained demonstrate a well-functioning immunosensor that responds to higher CA15-3 concentrations relevant to early cancer detection, and the selectivity performed showed negligible interference by other molecules present in blood plasma. Further improvements in this work may be achieved by convenient signal amplification approaches.

This work demonstrates a biosensor that can be used as a potentially autonomous device and still be able to detect relevant concentrations of cancer biomarkers and a response of interest for PoC analysis with high selectivity and reproducibility. This setup can be further improved for a point-of-care device by adding an electrochromic cell to indicate the presence and/or amount of the biomarker in the sample.

CRediT authorship contribution statement

Nádia S. Ferreira: Investigation, Methodology, Validation, Visualization, Formal analysis, Data curation, Writing – original draft. **Liliana P.T. Carneiro:** Investigation, Methodology, Validation, Formal analysis, Data curation, Writing – review & editing. **Alexandra M.F.R. Pinto:** Conceptualization, Supervision, Writing – review & editing. **M. Goreti F. Sales:** Conceptualization, Supervision, Funding acquisition, work administration, Writing – review & editing.

Declaration of competing interest

The authors declare that they have no known competing financial interests or personal relationships that could have appeared to influence the work reported in this paper.

Data availability

No data was used for the research described in the article.

Acknowledgements

The authors gratefully acknowledge the financial support of European Commission (FET-Open/H2020-Symbiotic/GA665046). Nádia S. Ferreira (Grant reference SFRH/BD/122955/2016), Liliana P. T. Carneiro (Grant reference SFRH/BD/122954/2016) and CEFT (UIDB/00532/2021 and UIDP/00532/2021) acknowledge Fundação para a Ciência e Tecnologia for financial support.

Appendix A. Supplementary data

Supplementary data to this article can be found online at https://doi.org/10.1016/j.biosx.2023.100344.

References

Akbari Nakhjavani, S., Khalilzadeh, B., Samadi Pakchin, P., Saber, R., Ghahremani, M.H., Omidi, Y., 2018. Biosens. Bioelectron. 122, 8–15. https://doi.org/10.1016/j.bios.2018.08.047.
Amani, J., Khoshroo, A., Rahimi-Nasrabadi, M., 2018. Microchim. Acta 185. https://doi.org/10.1007/s00604-017-2532-5.
Babu, K.R., Douglas, D.J., 2000. Biochemistry 39, 14702–14710. https://doi.org/10.1021/bi001265t.
Bayoumy, S., Hyytiä, H., Leivo, J., Talha, S.M., Huhtinen, K., Poutanen, M., Hynninen, J., Perheentupa, A., Lamminmäki, U., Gidwani, K., Pettersson, K., 2020. Commun. Biol. 3, 1–7. https://doi.org/10.1038/s42003-020-01191-x.
Berns, B.A., Torres, M.F., Oliveira, V.B., 2015. U.Porto J. Eng. 1, 89–103. https://doi.org/10.24840/2183-6493_001.001_0009.
Brodusch, N., Demers, H., Gauvin, R., 2018. J. Imaging 4, 88. https://doi.org/10.3390/jimaging4070088.
Carneiro, L.P.T., Ferreira, N.S., Tavares, A.P.M., Pinto, A.M.F.R., Mendes, A., Sales, M.G.F., 2021. Biosens. Bioelectron. 175, 1–9. https://doi.org/10.1016/j.bios.2020.112877.
Carneiro, L.P.T., Pinto, A.M.F.R., Mendes, A., Goreti, M., 2022. J. Electroanal. Chem. 906, 116009. https://doi.org/10.1016/j.jelechem.2022.116009.
Cerezo-Navarrete, C., Mathieu, Y., Puche, M., Morales, C., Concepción, P., Martínez-Prieto, L.M., Corma, A., 2021. Catal. Sci. Technol. 11, 494–505. https://doi.org/10.1039/d0cy02379e.
Chen, C., Wang, J., 2020. Analyst 145, 1605–1628. https://doi.org/10.1039/c9an01998g.
Desimoni, E., Brunetti, B., n.d.. Electroanalysis 25, 1645–1651. 2013. https://doi.org/10.1002/elan.201300150.
Di Nardo, F., Chiarello, M., Cavalera, S., Baggiani, C., Anfossi, L., 2021. Sensors 21, 5185. https://doi.org/10.3390/s21155185.
Dresselhaus, M.S., Jorio, A., Souza Filho, A.G., Saito, A.R., 2010. Phil. Trans. R. Soc. A 368, 5355–5377. https://doi.org/10.1098/rsta.2010.0213.
Ebeling, F.G., Stieber, P., Untch, M., Nagel, D., Konecny, G.E., Schmitt, U.M., Fateh-Moghadam, A., Seidel, D., 2002. Br. J. Cancer 86, 1217–1222. https://doi.org/10.1038/sj.bjc.6600248.
Fernández, A., Sinanoğlu, O., 1985. Biophys. Chem. 21, 163–166. https://doi.org/10.1016/0301-4622(85)80002-8.
Ferreira, N.S., Carneiro, L.P.T., Viezzer, C., Almeida, M.J.T., Marques, A.C., Pinto, A.M.F.R., Fortunato, E., Sales, M.G.F., 2022. J. Electroanal. Chem. 922. https://doi.org/10.1016/j.jelechem.2022.116710.
Ferreira, N.S., Sales, M.G.F., 2014. Biosens. Bioelectron. 53, 193–199. https://doi.org/10.1016/j.bios.2013.09.056.
Zhang, C., Zhang, D., Ma, Z., Han, H., 2019. Biosens. Bioelectron. 137, 1–7. https://doi.org/10.1016/j.bios.2019.04.049.
Gonzalez-Solino, C., Di Lorenzo, M., 2018. Biosensors 8, 11. https://doi.org/10.3390/bios8010011.
Globocan, 2020. Global Cancer Observatory. https://gco.iarc.fr/today/data/factsheets/cancers/20-Breast-fact-sheet.pdf. Assessed december 2022.
Hasanzadeh, M., Tagi, S., Solhi, E., Mokhtarzadeh, A., Shadjou, N., Eftekhari, A., Mahboob, S., 2018. Int. J. Biol. Macromol. 114, 1008–1017. https://doi.org/10.1016/j.ijbiomac.2018.03.183.
Hosseinzadeh, L, Fattahi, A, Khoshroo, A, 2022. A flexible paper-based electrochemical immunosensor towards detection of carbohydrate antigen 15-3. Anal. Bioanal. Electrochem. 14, 445–454.

Jawhari, T., Roid, A., Casado, J., 1995. Carbon N. Y. 33, 1561–1565. https://doi.org/10.1016/0008-6223(95)00117-V.
Khoshroo, A., Mazloum-Ardakani, M., Forat-Yazdi, M., 2018. Sensors Actuators, B Chem. 255, 580–587. https://doi.org/10.1016/j.snb.2017.08.114.
Kuntamung, K, Jakmunee, J, Ounnunkad, K, 2021. J. Mat. Chem. B 9, 6576–6585. https://doi.org/10.1039/D1TB00940K.
Liu, H., Song, C., Zhang, L., Zhang, J., Wang, H., Wilkinson, D.P., 2006. J. Power Sources 155, 95–110. https://doi.org/10.1016/j.jpowsour.2006.01.030.
Mahmoudi, T., de la Guardia, M., Baradaran, B., 2020. TrAC, Trends Anal. Chem. 125, 115842. https://doi.org/10.1016/j.trac.2020.115842.
Marques, R.C.B., Costa-Rama, E., Viswanathan, S., 2018. Sensors Actuators. B Chem. 255, 918–925. https://doi.org/10.1016/j.snb.2017.08.107.
Mehrotra, P., 2016. J. Oral Biol. Craniofacial Res. 6, 153–159. https://doi.org/10.1016/j.jobcr.2015.12.002.
Moretto, L.M., Kalcher, K., Editors, 2015. Environmental Analysis by Electrochemical Sensors and Biosensors. Elsevier. https://doi.org/10.1007/978-1-4939-1301-5.
Naresh, V., Lee, N., 2021. Sensors 21, 1–35, 10.3390/s21041109.
Nashner, M.S., Frenkel, A.I., Adler, D.L., Shapley, J.R., Nuzzo, R.G., 1997. J. Am. Chem. Soc. 119, 7760–7771. https://doi.org/10.1021/ja971039f.
Pasternak, G., Greenman, J., Ieropoulos, I., 2017. Sensor. Actuator. B Chem 244, 815–822. https://doi.org/10.1016/j.snb.2017.01.019.
Perfézou, M., Turner, A., Merkoçi, A., 2012. Chem. Soc. Rev. 41, 2606. https://doi.org/10.1039/c1cs15134g.
Rebelo, T.S.C.R, Ribeiro, J.A., Sales, M.G.F., Pereira, C.M., 2021. Sens. Bio-Sens. Res. 33, 100445. https://doi.org/10.1016/j.sbsr.2021.100445.
Saadati, A., Hassanpour, S., Hasanzadeh, M., Shadjou, N., Hassanzadeh, A., 2019. Int. J. Biol. Macromol. 132, 748–758. https://doi.org/10.1016/j.ijbiomac.2019.03.170.
Sales, M.G.F., Brandão, L., 2017a. Biosens. Bioelectron. 98, 428–436. https://doi.org/10.1016/j.bios.2017.07.021.
Shao, Q., 2014. J. Phys. Chem. B 118, 6175–6185. https://doi.org/10.1021/jp500280v.
Shawky, A.M., El-Tohamy, M., 2021. Mat. Chem. Phys. 272, 124983. https://doi.org/10.1016/j.matchemphys.2021.124983.
Soper, S.A., Brown, K., Ellington, A., Frazier, B., Garcia-Manero, G., Gau, V., Gutman, S. I., Hayes, D.F., Korte, B., Landers, J.L., Larson, D., Ligler, F., Majumdar, A., Mascini, M., Nolte, D., Rosenzweig, Z., Wang, J., Wilson, D., 2006. Biosens. Bioelectron. 21, 1932–1942. https://doi.org/10.1016/j.bios.2006.01.006.
Tavares, A.P.M., Ferreira, N.S., Truta, L.A.A.N.A., Sales, M.G.F., 2016. Sci. Rep. 6, 26132. https://doi.org/10.1038/srep26132.
Thompson, M., Ellison, S.L.R., Fajgelj, A., Willetts, P., Wood, R., 1999. Pure Appl. Chem 71, 337–348. https://doi.org/10.1351/pac199971020337.
Tothill, I.E., 2009. Semin. Cell Dev. Biol. 20, 55–62. https://doi.org/10.1016/j.semcdb.2009.01.015.
Truta, L.A.A.N.A., Moreira, F.T.C., Sales, M.G.F., 2018. Biosens. Bioelectron. 107, 94–102. https://doi.org/10.1016/j.bios.2018.02.011.
Wells, O.C., Gignac, L.M., Murray, C.E., Frye, A., Bruley, J., 2006. Scanning 28, 27–31. https://doi.org/10.1002/sca.4950280105.
Xu, W., Wu, Z., Tao, S., 2016. Energy Technol. 4, 1329–1337.https://doi.org/10.1002/ente.201600185.
Yamazaki, K., Iwura, T., Ishikawa, R., Ozaki, Y., 2006. J. Biochem. 140, 49–56. https://doi.org/10.1093/jb/mvj133.
Zhang, X., Chan, K.Y., 2003. Chem. Mater. 15, 451–459. https://doi.org/10.1021/cm0203868.